Estimations of Matching Layers Effects on Lens Antenna Characteristics

Phan Van Hung[1], Nguyen Quoc Dinh[1(✉)], Hoang Dinh Thuyen[1], Nguyen Tuan Hung[1], Le Minh Thuy[2], Le Trong Trung[3], and Yoshihide Yamada[4]

[1] Le Quy Don Technical University, Hanoi, Vietnam
dinhnq@mta.edu.vn
[2] School of Electrical Engineering,
Hanoi University of Science and Technology, Hanoi, Vietnam
[3] Telecommunications University, Nhatrang, Vietnam
[4] Malaysia-Japan International Institute of Technology UTM, Kuala Lumpur, Malaysia

Abstract. The dielectric lens antenna is a prime candidate for the mm-wave 5G communications system. The size and the radiation efficiency can be improved by using a high-density dielectric lens antenna. However, the dense dielectric material lenses can make some antenna properties deteriorate due to the reflections at the surface between the air and the dielectric. These unexpected effects can be solved by using a quarter-wavelength matching layer (ML). In this paper, the authors perform the study to estimate the influence of the ML on the antenna properties on specific dielectric materials. The results illustrate a marked improvement in gain, a significant reduction in the side-lobe level, and considerable changes in the electric field distribution on the plane with and without using the ML. Besides, the article also shows the abilities to minimize the antenna size when different types of dielectric materials are chosen while maintaining the antenna radiation characteristics.

Keywords: Lens antenna · Matching layer · Quarter-wavelength matching

1 Introduction

At the millimeter-wave frequency, the antenna element size becomes smaller ten times compared to the sub-6 GHz 5G base station antenna element. This frequency range allows selecting various antennas elements such as lens, array, and reflector antennas [1–4]. Reflector antennas with multiple feeds have high direction and the ability to create multi-beams. However, high cross-polarization and the side-lobe level if these antennas are affected by feeds [5].

In recent years, there has been an increased interest in using dielectric lens antennas among researchers and manufacturers [6–10]. This type of antenna is capable of producing multi-beams and broadband. With a unique structure, the lens antenna is not affected by the blockage of the reflectors and the feeds. Besides, the lens antenna allows electric waves from the front to penetrate backwards. Lens antennas have been studied

N.-S. Vo and V.-P. Hoang (Eds.): INISCOM 2020, LNICST 334, pp. 85–94, 2020.
https://doi.org/10.1007/978-3-030-63083-6_7

and applied to many kinds of broadband communication systems such as Ka-band [11], Q band [12], and V band [13], automotive cruise control radars and obstacle detection radars in W band [14, 15], in which lenses made of the dielectric materials, uniform size and shape are designed according to the system specifications.

In dielectric lens antenna applications, choosing the relative permittivity of the lens material is very important since its value has a major influence on the antenna radiation characteristics. Dielectric lens antennas made of dense dielectric materials like Mica, Alumina, and Silicon enhance the efficiency of transmitting energy through the lens and improve the front to back radiation ratio of the antenna. However, the dense dielectric material in the lens antenna causes reflection from the lens surface between the air and the dielectric layer of the lens. The reflection can significantly affect not only the input impedance of the power [16–18] but also the characteristics of lens antennas such as reduced gain, beam distortion, and increased side-lobe level. Therefore, the ML is applied to lessen these unwanted effects, thereby improving the efficiency of using the lens antenna in information systems [19, 20]. There are two fundamental methods to create a ML: using a quarter-wavelength matching layer and the reaction wall which are studied by Morita, S.B. Cohn in [21, 22].

However, up to now, the studies of effects of high-density dielectric materials used to make typical lenses such as Teflon, Mica, Alumina, and Silicon have not been conducted yet. In this paper, the authors perform a theoretical calculation of the power reflection coefficient and the simulation in the electromagnetic environment, thereby making accurate evaluations of the specific impact of each dielectric material type. The results serve as a basis for the selection of specific materials in the manufacture of lens antennas. The paper includes 4 parts: part 2 presents the theoretical calculations of the quarter-wavelength matching layer, constructing antenna models and simulation parameters. The results and the discussion are shown in part 3. The conclusion is presented in part 4.

2 Theoretical Matching Layers and Antenna Modeling

2.1 Theoretical Matching Layers

The relative effectiveness of the ML technique can be easily assessed by the power reflection coefficient at the surface between the air and the dielectric. In Fig. 1c, the ML is assigned between the air and the dielectric region: region 1 denotes the air, region 2 is the ML and region 3 denotes the dielectric. The power reflection coefficient at the surface between region i and region j is denoted as r_{ij}. Accordingly, r_{12} and r_{23} are the power reflection coefficients at the surface between Regions 1 and 2 and Regions 2 and 3, respectively. The power reflection coefficient is determined by the following equation [23, 24].

$$r_{ij} = \left| \frac{\sqrt{\varepsilon_i} - \sqrt{\varepsilon_j}}{\sqrt{\varepsilon_i} + \sqrt{\varepsilon_j}} \right| \tag{1}$$

$$R = \frac{(r_{12} + r_{23})^2 - 4r_{12}r_{23}sin^2\alpha_2 d}{(1 + r_{12}r_{23})^2 - 4r_{12}r_{23}sin^2\alpha_2 d} \tag{2}$$

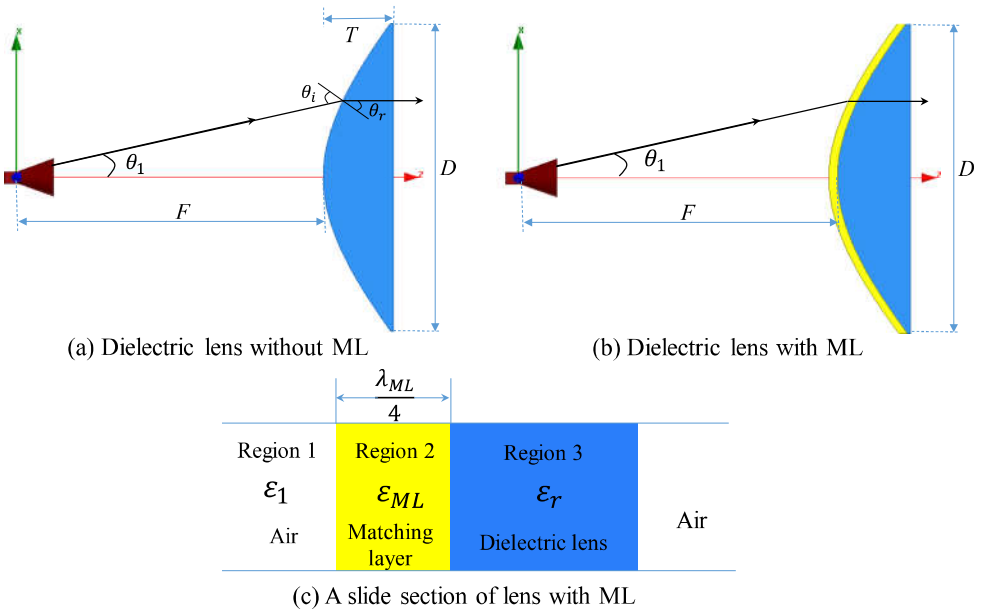

Fig. 1. Antenna modeling of a dielectric lens antenna

where $\alpha_2 = 2\pi/\lambda_{ML}$, λ_{ML} is the wavelength in the ML environment. If ε_{ML} is between the value of ε_1 and ε_r, then $r_{12}r_{23}$ is positive, thereby R changes and serves as a function of ML layer thickness d. Therefore, R reaches the minimum value when $d = \lambda_{ML}/4$ and equals zero when $r_{12} = r_{23}$, then ε_{ML} is the geometric mean of ε_1 and ε_r or $\varepsilon_{ML} = \sqrt{\varepsilon_1\varepsilon_r}$.

The thickness of the ML layer is defined as follows:

$$d = \frac{\lambda_{ML}}{4} = \frac{\lambda}{4\,n_{ML}} \tag{3}$$

where λ is the wavelength in free space and n_{ML} is the refraction index of ML. Under these conditions, all power is transferred from the medium (1) into the environment (2), no power is reflected at the surface. Besides, assigning ML to a quarter wavelength with an appropriate dielectric constant also aims to coordinate the impedance at the surface of the two power lines.

2.2 Antenna Modeling

As can be seen in Fig. 1, the lens antenna structure consists of a conical horn antenna as a wide-angle power and a lens which has a simple structure of a curved surface and a flat surface and rotates around the oz axis. The conical horn antenna is designed to perform at 28 GHz and reaches a maximum gain of 15.15 dBi. The lenses are dense dielectric materials with a relative permittivity of $\varepsilon_r = 2.1$ (Teflon), $\varepsilon_r = 5.7$ (Mica), $\varepsilon_r = 9.2$ (Alumina) and $\varepsilon_r = 11.9$ (Silicon), respectively. These materials are commonly used in the design and manufacture of lens antennas. The lens surface curves towards the feed horn. The focal point of the lens is located at the center of the horn antenna, which is the interface between the waveguide and the flare of the conical horn. The curved surface of the lens is hyperbolic, and it is determined by Eq. (4) [25–27]. The diameter of the lens is D. F is a distance from the focal point to the lens vertex. The lens is located at

the angles of $\theta_{1Max} = \pm 25.545^0$, where the electromagnetic field of the conical horn antenna is −10 dB compared to the maximum values.

$$r = \frac{(n-1)F}{ncos\theta_1 - 1} \tag{4}$$

The lens thickness at the center is calculated as:

$$T = \frac{1}{n+1}\left[\sqrt{F^2 + \frac{(n+1)D^2}{4(n-1)}} - F\right] \tag{5}$$

where r is the distance from the focal point to the curved surface of the lens. θ_1 is the angle created by the ray from the focal point to the curved surface of the lens and the optical axis in region 1, and n is the refractive index of the lens. θ_i and θ_r represent the incident angle and the refractive angle at the lens surface. These angles satisfy Snell's law.

$$n = \frac{sin\theta_i}{sin\theta_r} \tag{6}$$

The lens is covered with a quarter-wavelength matching layer whose structure is shown in Fig. 1b. In Fig. 1c, The ML has the relative permittivity (ε_{ML}) and the thickness ($d = \lambda_{ML}/4$), in which λ_{ML} is the wavelength inside the ML. The ML is set in region 2 (between region 1 and region 3). The rays are radiated from the conical horn antenna in region 1, passing through the quarter-wavelength matching layer to region 3, and then going through the other side of the lens forming the rays parallel to the oz axis.

2.3 Simulation Parameters

The simulation parameters, computer configurations, and software are shown in Table 1. The survey is conducted using the ANSYS HFSS electromagnetic field simulation software. A simultaneous setting of two adaptive cross approximation (ACA) and multi-pole multi-level fast method (MLFMM) are employed to analyze results to improve accuracy as well as save memory and calculation time.

Table 1. Simulation parameters

Computer specifications	CPU	Intel (R) 3.20 GHz
	RAM	32 GB
	Software	ANSYS HFSS
	Simulation method	MLFMM and ACA

(*continued*)

Table 1. (*continued*)

Dielectric lens material parameters	Lens diameter [mm]	D	100
	Distance from the origin to the lens vertex [mm]	F	100
	Teflon relative permittivity	ε_r	2.1
	Mica relative permittivity		5.7
	Alumina relative permittivity		9.2
	Silicon relative permittivity		11.9
	Air relative permittivity	ε_1	1
	ML relative permittivity	ε_{ML}	$\sqrt{\varepsilon_1 \varepsilon_r}$
	Matching layer thickness [mm]	d	$\lambda_{ML}/4$
Survey frequency			28 GHz

3 Simulation Results

3.1 Power Reflection Coefficients

Figure 2 shows the effects of the thickness and relative permittivity of the ML on the power reflection coefficients of the lens antennas. Obviously, when the thickness of ML is equal to a quarter of the wavelength in ML medium, the power reflection coefficient is lowest. When the relative permittivity of the ML is equal to the geometric mean of the air and the dielectric substance of the lens and the thickness of ML is equal to a quarter of the wavelength in ML medium, the power reflection coefficient is zero, as illustrated in Fig. 2a. When the thickness of the ML layer changes, the power reflection coefficient at the interface of the air layer and the dielectric of the Silicon lens is always higher than

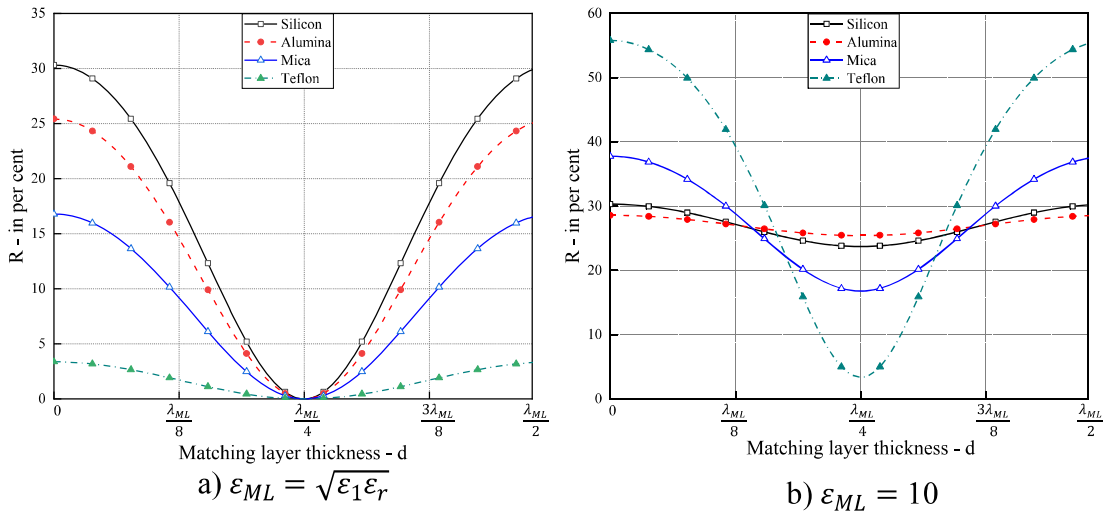

Fig. 2. Power reflection coefficients

that of other dielectric materials. The power reflection coefficient is even 30% higher when the thickness of the ML is zero or half the wavelength in the ML medium. In Fig. 2b, a relative permittivity value of the ML ($\varepsilon_{ML} = 10$) is randomly surveyed. The results show that the power reflection coefficient is minimized when $d = \lambda_{ML}/4$ and cannot eliminate the reflected energy at $\varepsilon_{ML} \neq \sqrt{\varepsilon_1 \varepsilon_r}$. The results show the accuracy of the theoretical calculation.

3.2 Radiation Patterns

The radiation pattern of the lens antenna with and without the ML using the different materials are presented in Fig. 3. It is easily observed that the antenna lens radiations with the ML is better than those of the ML-free antenna. Specifically, in the absence of the ML, the lens antenna has the highest gain of 27.07 dBi when Teflon is used as a dielectric, and it reaches the highest gain of 25.39 dBi when the lens dielectric is Mica. In the presence of the ML, the lens antenna has the highest gain of 27.82 dBi with the dielectric of Silicon, and 27.14 dBi with the dielectric of Mica. In Silicon dielectric, the maximum gain with the ML is 2.2 dB higher than the maximum gain without the ML, while in Teflon dielectric this figure is only 0.32 dB.

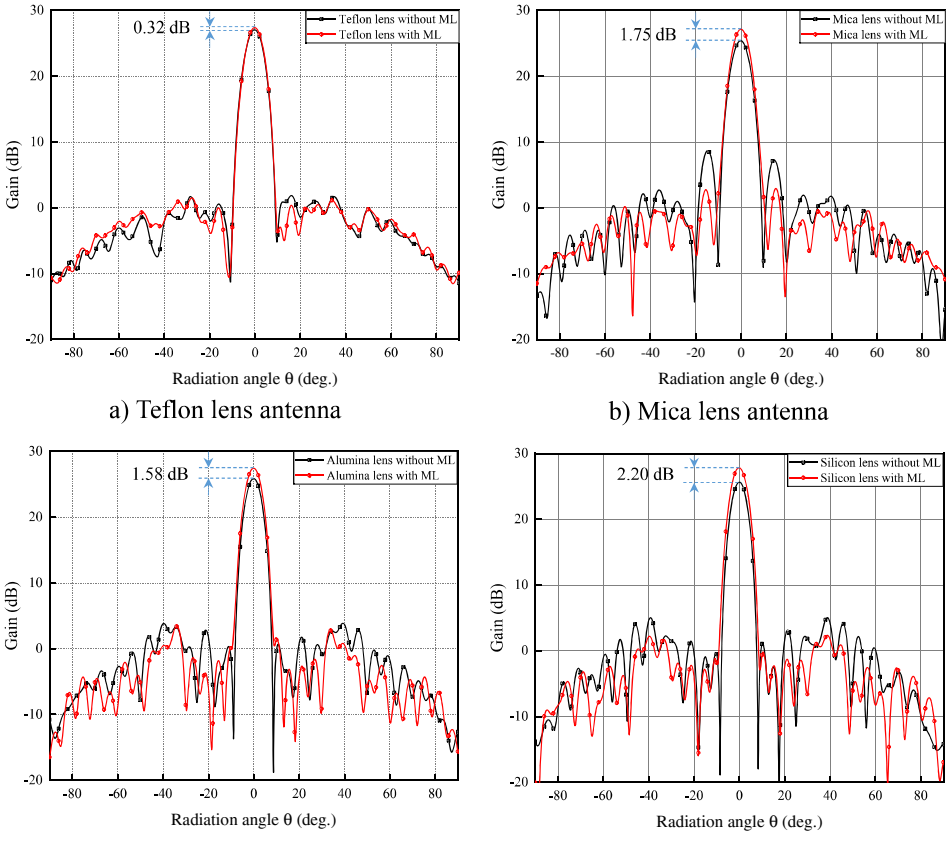

Fig. 3. Radiation patterns of different materials with and without matching layers.

3.3 Side-Lobe Levels

The changes in the gains and the side-lobe levels when using and not using the ML in the different dielectrics are shown in Fig. 4. As shown in the graph, when the ML is attached to the lens, the side-lobe levels of all four cases decrease. Mica reduces by 7.52 dB, from −16.69 dB to −24.21 dB, followed by Silicon dielectric and Alumina at 5 dB and 1.99 dB, respectively; whereas in the case of Teflon dielectric, there is a minor change in the side-lobe level (only 0.68 dB, from −25.21 dB to 25.89 dB).

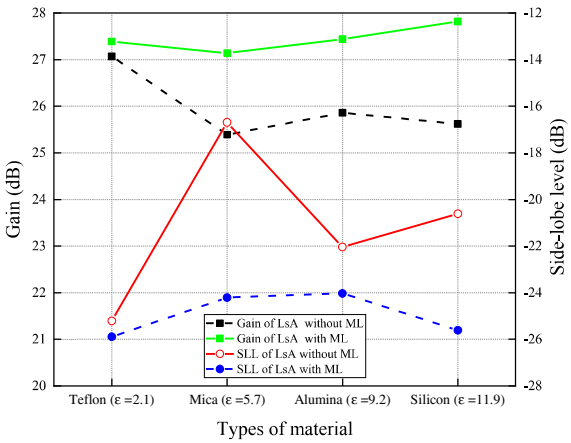

Fig. 4. The comparison of the gains and the side-lobe levels.

3.4 The Lens Thickness

The specific simulation results and calculations are presented in Table 2. Applying formula (5) and established simulation parameters, we can calculate the thickness of the lens. Accordingly, the lens with the Teflon dielectric is the thickest with 25.17 mm, while the lens with the Silicon dielectric is the thinnest with only 7.07 mm. The thicknesses of Alumina and Mica are 8.07 mm and 10.67 mm, respectively.

Table 2. Comparison results.

Types of material	lens without ML				Lens with ML			
	Gain [dBi]	SLL [dB]	HPBW [deg.]	Lens thickness [mm]	Gain [dBi]	SLL [dB]	HPBW [deg.]	Lens thickness [mm]
Teflon (ε_r = 2.1)	27.07	−25.21	7.42	22.94	27.39	−25.89	7.29	25.17
Mica (ε_r = 5.7)	25.39	−16.69	7.39	8.94	27.14	−24.21	7.16	10.67
Alumina (ε_r = 9.2)	25.86	−22.04	6.77	6.53	27.44	−24.03	6.84	8.07
Silicon (ε_r = 11.9)	25.62	−20.61	6.54	5.63	27.82	−25.61	6.84	7.07

3.5 Electric Field Distributions

Figure 5 shows the electric field distributions of the lens antennas with the dielectric Teflon and Silicon on the xz plane. From Fig. 5c and d, it is easily to see the differences in the electric field distributions between the Silicon antenna lens without the ML (5c) and with the ML (5d). As for the Silicon lens without the ML, the electric field distribution between the lens and the conical horn antenna is rough, even cancels out just before the lenses, and the spherical waveform of the feed horn is no longer clear. As for ML-coated Silicon lens, the field distribution is quite smooth and more uniform, and the planar waves behind the lens are shown more clearly. The first reason for this field distribution is that silicon has a dense dielectric structure; hence, the rays from the feed horn to the lens surface are reflected more. Another possible explanation is that the curvature of the inner surface of the lens is less than that of Teflon; therefore, the rays bounce back toward the feed horn more. Accordingly, the field distribution on the xz plane of the Teflon lens antenna undergoes a minor change on account of Teflon having a less dense dielectric structure and a higher curvature of the inner surface of the lens, thus the rays are reflected from the surface less and are deflected into the edge of the lens instead of being reflected toward the feed horn, as shown in Fig. 5a and b. This result shows the efficiency of using the ML for dense dielectric structure materials.

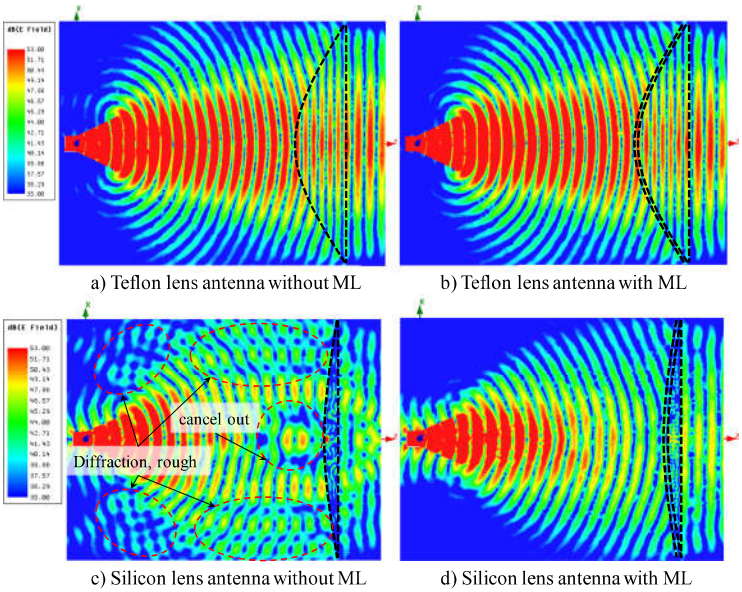

Fig. 5. Electric field distributions on the xz plane.

The above-mentioned results show the effectiveness of ML in improving the radiation ability of lens antennas, a significant reduction in the side-lobe level, and a more uniform distribution of the electric field. Besides, the results also show the corresponding sizes of the lenses. This will be helpful for researchers, designers, and manufacturers to select an appropriate lens antenna structure with a smaller size and better properties.

4 Conclusion

Through the simulation, analysis, and evaluation results, this paper has demonstrated the role of ML in improving the characteristics of a specific dense dielectric lens. The results show that covered with a ML, the Silicon dielectric can improve the maximum gain of 2.2 dB while the Mica dielectric can reduce the maximum side-lobe level of 7.52 dB. In addition, the Silicon dielectric lens is 18.1 mm thinner than the Teflon dielectric lens and achieves a higher gain. These results show the efficiency of using a ML for high-density dielectric lens antennas.

Acknowledgments. This research is funded by Vietnam National Foundation for Science and Technology Development (NAFOSTED) under grant number 102.04-2018.08.

References

1. Dinh, N.Q., Binh, N.T., Yamada, Y., Michishita, N.: Proof of the density tapering concept of an unequally spaced array by electric field distributions of electromagnetic simulations. J. Electromag. Waves Appl. **34**(5), 668–681 (2020). https://www.tandfonline.com/doi/full/10.1080/09205071.2020.1736185
2. Yamada, Y., et al.: Unequally element spacing array antenna with butler matrix feed for 5G mobile base station. In: 2nd International Conference on Telematics and Future Generation Networks (TAFGEN), pp. 72–76. Kuching, Malaysia (2018)
3. Quzwain, K., Yamada, Y., Kamardin, K., Rahman, N.H.A., Dinh, N.Q.: Reflector surface shaping method for a Cassegrain antenna, In: 6th International Conference on Space Science and Communication, pp. 1–5. Johor, Malaysia (2019)
4. Tajima, T., Yamada, Y.: Design of shaped dielectric lens antenna for wide angle beam steering. Electron. Commun. Japan Part 3, **89**(2), 1–12 (2006)
5. Hong, W., et al.: Multibeam antenna technologies for 5G wireless communications. IEEE Trans. Antennas Propag. **65**(12), 6231–6249 (2017)
6. Filipovic, D.F., Gearhart, S.S., Rebeiz, G.M.: Double-slot antennas on extended hemispherical and elliptical silicon dielectric lenses. IEEE Trans. Microw. Theory Tech. **41**(10), 1738–1749 (1993)
7. Costa, J.R., Fernandes, C.A., Godi, G., Sauleau, R., Le Coq, L., Legay, H.: Compact ka-band lens antennas for LEO satellites. IEEE Trans. Antennas Propag. **56**(5), 1251–1258 (2008)
8. Pasqualini, D., Maci, S.: High-frequency analysis of integrated dielectric lens antennas. IEEE Trans. Antennas Propag. **52**(3), 840–847 (2004)
9. Hung, P.V., Dinh, N.Q., Nguyen, T.V.D., Yamada, Y., Michishita, N., Islam, M.T.: Electromagnetic simulation method of a negative refractive index lens antenna. In: 2019 International Conference on Advanced Technologies for Communications (ATC), pp. 109–112. Hanoi, Vietnam (2019)
10. Nguyen, N.T., Sauleau, R., Ettore, M., Le Coq, L.: Focal array fed dielectric lenses: an attractive solution for beam reconfiguration at millimeter waves. IEEE Trans. Antennas Propag. **59**, 2152–2159 (2011)
11. Wu, X., Eleftheriades, G.V., Van Deventer Perkins, T.E.: Design and characterization of single- and multiple-beam mm-wave circularly polarized substrate lens antennas for wireless communications. IEEE Trans. Microw. Theory Tech. **49**, 431–441 (2001)
12. Barès, B., Sauleau, R.: Electrically small shaped integrated lens antennas: a study of feasibility in Q-band. IEEE Trans. Antennas Propag. **55**, 1038–1044 (2007)

13. Holzman, E.L.: A highly compact 60-GHz lens-corrected conical horn antenna. IEEE Antennas Wirel. Propag. Lett. **3**, 280–282 (2004)
14. Schoenlinner, B., Wu, X., Ebling, J.P., Eleftheriades, G.V., Rebeiz, G.M.: Wide-scan spherical-lens antennas for automotive radars. IEEE Trans. Microw. Theory Tech. **50**, 2166–2175 (2002)
15. Migliaccio, C., Dauvignac, J.Y., Brochier, L., Le Sonn, J.L., Pichot, C.: W-band high gain lens antenna for metrology and radar applications. Elect. Lett. **40**(22), 1394–1396 (2004)
16. Van der Vorst, M.J.M., et al.: Effect of internal reflections on the radiation properties and input impedance of integrated lens antennas – Comparison between theory and measurements. IEEE Trans. Microw. Theory Tech. **49**, 1118–1125 (2001)
17. Godi, G., Sauleau, R., Thouroude, D.: Performance of reduced size substrate lens antennas for millimeter-wave communications. IEEE Trans. Antennas Propag. **53**, 1278–1286 (2005)
18. Neto, A., Maci, S., De Maagt, P.J.I.: Reflections inside an elliptical dielectric lens antenna. IEE Proc. Microw. Antennas Propag. **145**(3), 243–247 (1998)
19. Nguyen, N.T., Sauleau, R., Martinez, P.: Very broadband extended hemispherical lenses: role of matching layers for bandwidth enlargement. IEEE Trans. Antennas Propag. **57**, 1907–1913 (2009)
20. Tokan F.: Matching layer design procedure for a novel broadband dielectric lens antenna, pp. 149–198 (2013). ISBN 978-0-9891305-3-0 ©2013 SDIWC (2013)
21. Morita, T., Cohn, S.B.: Simulated quarter-wave matching sheet: In: U.R.S.I. Meeting, Washington D. C. (1954)
22. Morita, T., Cohn, S.B.: Microwave lens matching layer by simulated quarter-wave transformer. IRE Trans. Antennas Propag. **4**(1), 33–39 (1956)
23. Jones, E.M.T., Cohn, S.B.: Surface matching of dielectric lens. J. Appl. Phys. **26**(4), 452–457 (1955)
24. Stratton, J.A.: Electromagnetic Theory. McGraw-Hill Book Company Inc., New York (1941)
25. Lo, Y.T., Lee, S.W.: Antenna Handbook, 2nd edn. Van Nostrand Rainhold Company, New York (1988)
26. Tajima, Y., Yamada, Y.: Design of shaped dielectric lens antenna for wide angle beam steering. Electron. Commun. Japan Part 3 **89**(2), 1–12(2006)
27. Sliver, S.: Microwave Antenna Theory and Design. McGraw-Hill Inc., New York (1949)